Adsorption (2011) 17:701–721
DOI 10.1007/s10450-011-9355-1

Multi-component adsorptive separation: use of lumping in PSA process simulation

Pramathesh R. Mhaskar · Arun S. Moharir

Received: 20 September 2010 / Accepted: 1 March 2011 / Published online: 18 March 2011

Abstract Being a discrete-continuous process, approach to a cyclic steady state in computer simulation of Pressure Swing Adsorption is through iterative procedures and simulation itself is quite computation-intensive. Considering the fact that simulation based design itself is an iterative process, it is imperative that simulation be computationally very efficient and phenomenologically as close to the physics of adsorption-desorption as possible. Utility of lumping the components of a gas mixture into fewer pseudo-components was computationally examined in the simulation of a representative multi-step cycle of a pressure swing based adsorptive separation process applied to natural gas treatment. The actual feed had six components competing for adsorbent sites. Five different lumping alternatives were studied and compared with the simulation results for a full six-component simulation under identical equipment dimensions and operating conditions. Lumping could reduce the number of equations to be solved by more than half and the corresponding reduction in CPU time was about 90%. The six component mixture of Natural Gas was found to be sufficiently represented by two pseudo-components. The predicted recovery (in terms of Methane and Ethane) and quality (in terms of content of higher hydrocarbons) of the raffinate differed by not more than 0.8% and 0.02% respectively. The paper discusses possible heuristics for decision-making regarding appropriate lumping as verified by extensive simulation studies.

P.R. Mhaskar · A.S. Moharir (✉)
Department of Chemical Engineering, IIT Bombay, Powai, Mumbai 400076, India
e-mail: amoharir@iitb.ac.in

P.R. Mhaskar
e-mail: prmhaskar@iitb.ac.in

Keywords Lumping into pseudo-components · Adsorptive separation · Natural gas treatment · Simulation · Pressure-swing · Heuristics

Nomenclature

A	Cross sectional area of the column, m^2
b_i	Adsorption equilibrium constant for ith component on the solid surface at the operating temperature, m^3/mole
C_v	Valve coefficient, dimensionless
d_p	Diameter of a spherical adsorbent particle or equivalent diameter for a non-spherical particle, m
ε	External voidage in the bed packed with the adsorbent particles, dimensionless
Φ	Sphericity factor of the adsorbent particle
dt	Step size for temporal discretization, s
dz	Step size for spatial discretization, m
L	Height of the adsorbent layer packed inside the column, m
MW_i	Molecular weight of ith component, kg/kmole
P	Absolute Pressure, Pa(a)
Q_{Feed}	Volumetric feed rate of feed Natural Gas at standard conditions, m^3/hr at STP conditions
q_i	Average concentration of ith component adsorbed in the volume of adsorbent particles, moles/m^3 solid
$q_{i\max}$	Maximum monolayer adsorption capacity of ith component on the adsorbent surface, moles/m^3 solid
R	Ideal Gas Law constant, Pa·m^3/mole/K
t	Temporal coordinate, s
T	Operating temperature, K
t_{cycle}	Total cycle time, s
t_s	Staggering time, s

u	Superficial velocity of the fluid, m/s
y_i	Fluid phase mole fraction of ith component, dimensionless
z	Spatial coordinate, m

Abbreviations

C_1	Methane
C_{1+}	Ethane and higher alkanes
C_2	Ethane
C_{2+}	Propane and higher alkanes
C_3	Propane
C_4's	i-Butane + n-Butane
CSS	Cyclic steady state
IAST	Ideal Adsorbed Solution Theory
i-C_4	i-Butane or Isobutane
g	Gas phase
l	Liquid phase
N_B	Number of Beds
n-C_4	n-Butane or Normal Butane
N_{max}	Maximum number of components in the system
N_{PC}	Number of pseudo-components
N_r	Number of lumping rules applied
N_s	Number of steps in the cycle
PSA	Pressure Swing Adsorption
PVSA	Pressure Vacuum Swing Adsorption
scf	Supercritical fluid phase
SCMPH	Standard cubic metres per hour
SMB	Simulated Moving Bed
STP	Standard Conditions of Temperature and Pressure, 10^5 Pa absolute and 273.15 K
TSA	Temperature Swing Adsorption
VSA	Vacuum Swing Adsorption

1 Introduction

Separation of multi-component feed streams into their components is a frequently encountered task in process industry. Multi-component streams are also involved in reactions. Components of 'continuous' mixtures like Crude Oil or Coal or Polymers have been grouped into pseudo-components for ease of calculations involved in their reactions and separations (Aris and Gavalas 1966; Aris 1989; Glinos and Malone 1984; Chou and Prausnitz 1986; Jacome et al. 2005). Lumping philosophy is also used successfully for capturing the essence of complicated mass transfer processes (Sircar and Hufton 2002). Experimental difficulties compel the analyst to report compositions of natural gas mixtures in terms of pseudo-components formed by lumping two or more number of components (Brown et al. 2009).

For adsorptive separation processes, both pure component and mixture adsorption data are very scarce. In case of adsorption based removal of trace components from a mixture, experimental measurement of the data at very low adsorbate concentrations with sufficient accuracy is a severe problem (Rege and Yang 2001). Experimentally verified data on multi-component adsorption equilibrium, kinetics and heats of adsorption for mixtures having three and more components is relatively more difficult to get compared to the same data for pure components and binary mixtures (Reverchon et al. 1998; Sircar 2006).

Multi-component adsorption also poses challenges on the simulation front. Mathematical modeling of just the adsorption breakthrough curves for a system having more than four components had numerical problems related to stability, convergence and physical reliability of the results (Reverchon et al. 1998). Computational platforms and operating systems have memory limitations. These shortcomings point to the need to simplify the mathematical models and examine the behavior after incorporating lumping strategy in the simulation of a variety of adsorptive separations. Overall terms such as Biochemical Oxygen Demand (BOD) or Total Organic Carbon (TOC), have been used in waste-water treatment but grouping the components into more than one pseudo-component was shown to be a more viable approach (Calligaris and Tien 1982).

In this work, component lumping based simulation of a representative Natural Gas (NG) treatment by using pressure swing adsorption cycle is considered as a case.

2 Natural gas treatment by using PSA

NG Treatment based on PSA and using Silica Gel adsorbent is a commercially operated process used to recover Propane, Butane isomers, n-Pentane, etc. from the feed and provide a predominantly Methane and Ethane containing stream to downstream processes like the manufacture of Synthesis Gas (Maurer 1992; Robben and O'Brien 2005; Daiminger et al. 2006). The higher hydrocarbons in NG could cause coking in the downstream reactors and their removal is an important feed treatment step in such cases. Part of our work reported here was for development and deployment of a PSA process for such natural gas treatment.

In this work, the six components ($N_{max} = 6$) considered in the feed NG are Methane, Ethane, Propane, n-Butane, i-Butane and Carbon Dioxide as were reported for an industrial source. The PSA system belongs to the type of adsorption process in which the desired product is the most weakly adsorbed component and its quality is perceived in terms of extent of reduction in the relatively strongly adsorbed components. More specifically, in the present technology development task, the objective was to recover as much Methane and Ethane from the Natural Gas as possible with as less higher hydrocarbons in the raffinate as possible.

Table 1 Steps ($N_s = 5$), their sequence and valve status for PSA cycle on NG treatment

Step	Description	Feed valve	Raffinate valve	Extract valve	Purge valve
1	Pressurization by feed gas	On	Off	Off	Off
2	High pressure adsorption of feed gas	On	On	Off	Off
3	Co-current depressurization	Off	On	Off	Off
4	Counter-current depressurization	Off	Off	On	Off
5	Counter-current purge by fraction of raffinate	Off	Off	On	On

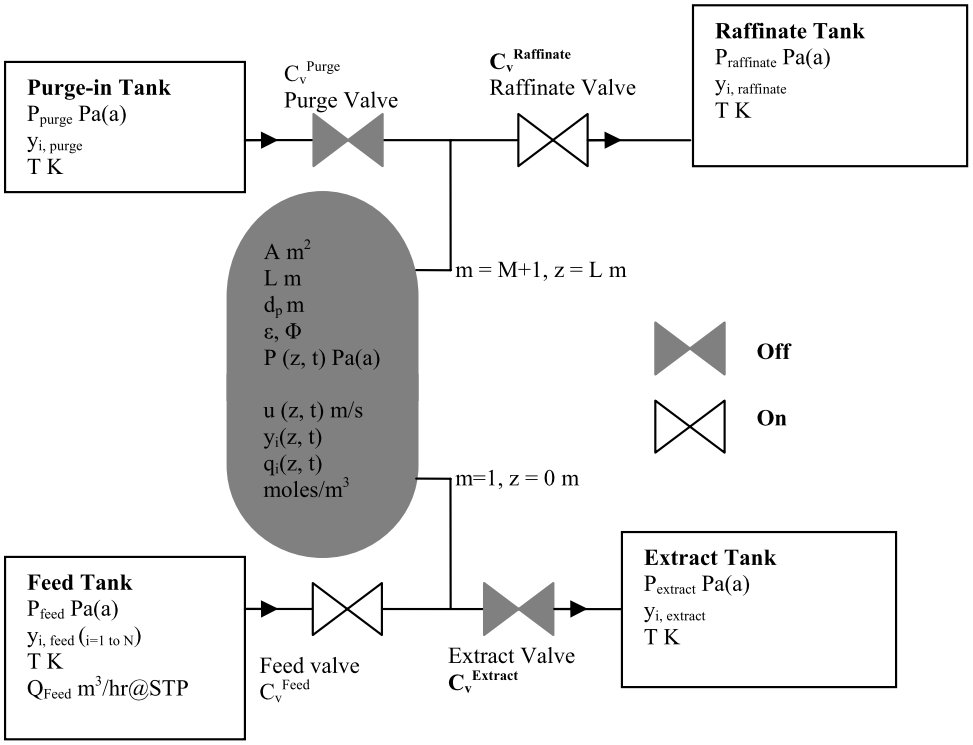

Fig. 1 State of a bed in the step of high pressure adsorption of feed gas

The adsorbent considered was a special variety of mesoporous Silica Gel which has increasing affinity for hydrocarbons of higher carbon number. The order of physical adsorption of the components of NG mixture on the surface of this adsorbent is such that the alkane with the highest number of Carbon atoms will be the most strongly adsorbed, that with the lowest number of Carbon atoms will be the most weakly adsorbed and CO_2 is also adsorbed due to the presence of double bonds (Olivier and Jadot 1997).

2.1 Description of a typical process cycle

The steps used in the PSA cycle for this system are typical of the ones in which raffinate is the desired product. In this specific process, the raffinate is designated as 'Lean' gas and the extract as 'Rich' gas. Compared to their mole fraction in the feed NG, the Lean gas or the raffinate has higher mole fraction of the weakly adsorbed components and the Rich gas or the extract has higher mole fraction of the strongly adsorbed components. For continuous production, more than one bed is used wherein each bed has to complete the same step sequence of the cycle before proceeding to a next cycle. The beds operate with a phase lag ($t_s = t_{cycle}/N_B$) in implementing the PSA cycles as in any PSA process. After completion of a number of cycles, all the beds attain a cyclic steady state (CSS). Modeling the behavior of a single bed is sufficient to understand and design a process. Table 1 gives the sequence of operating steps of a full PSA cycle to which each bed is subjected and the valve status in each of these steps. Figure 1 shows a bed in adsorption step along with the associated valves and tanks (reservoirs for various feed and product streams held at constant pressures) for a feed rate of Q_{Feed} m^3 per hour at STP conditions. Similar depiction can be envisaged for the bed in other steps by using Table 1.

At start-up, the bed is assumed to be at the pressure of extract tank and contains pure CH_4 (most weakly adsorbed component) in both the phases. For the lumped cases, at

start up, the bed is assumed to be filled with 1st pseudo-component. The adsorbed phase and the bulk phase are assumed to be in adsorption equilibrium at this pressure. After the first cycle, the initial conditions of the bed are the conditions of the bed at the end of the last step of the first cycle. The initial conditions for any step are the conditions at the end of the previous step in the cycle. Stepwise description is given as follows:

Step 1: Pressurization of the bed with feed NG mixture (duration $= t_1$ s)
The bed pressure is much lower than the feed tank pressure. The valve connecting the feed tank to the bed is opened. The other valves are closed. The bed starts getting pressurized and at the end of this step, the bed is pressurized to a value nearly equal to the feed tank pressure. Simultaneous adsorption that takes place, is considered in the PSA process model.

Step 2: High pressure adsorption of the feed NG mixture (duration $= t_2$ s)
The valve connecting the raffinate tank to the bed is opened at the start of this step. Since the raffinate tank pressure is less than that of the pressurized bed, material starts flowing out from the bed to the raffinate tank. This tank collects a gas that is mostly free of Propane and higher alkanes and Carbon Dioxide as these components get preferentially adsorbed in the adsorbent. Pressure in the bed remains reasonably constant in this step except developing small pressure drop across the bed.

Step 3: Co-current depressurization of the bed (duration $= t_3$ s)
At the start of this step, the feed tank connection is closed and the weaker adsorbates that may be trapped in the void space of the bed are released into the raffinate tank. Desorption of the species will also occur simultaneously with depressurization and the model considers it. This step is included to improve the recovery of the process.

Step 4: Counter-current depressurization of the bed (duration $= t_4$ s)
At the start of this step, the raffinate tank connection is closed and the extract tank connection is opened. The extract tank is at a much lower pressure than the bed pressure. The bed starts depressurizing counter-currently. Desorption takes place further as the pressure decreases again. The desorbed gas is collected in the extract tank.

Step 5: Counter-current purge with fraction of the raffinate (duration $= t_5$ s)
Some fraction from the raffinate tank is used for purging counter-currently the already depressurized bed. The purge tank is at a higher pressure than the depressurized bed. The valve connecting the purge tank to the bed is opened at the start of this step. The purge gas enters the bed and starts flowing counter-currently through the bed. This step is used to flush the desorbed heavy components in the void spaces. The outgoing stream from this step is also collected in the extract tank. One cycle is completed at the end of this step (at $t_1 + t_2 + t_3 + t_4 + t_5 = t_{\text{cycle}}$) and the bed executes Step 1 of the next cycle.

3 PSA simulation model

In this work, all the computations have been done using our own generic simulator for PSA processes and more details of the model will be published in near future. The heats of sorption of the NG mixture components are low and interactions with the adsorbent are not strong enough to consider non-isothermal model. The data on mass transfer coefficients for all the six components on this adsorbent was not available. The main assumptions for this work are isothermal operation, use of Extended Langmuir isotherm for describing the multi-component adsorption equilibria, use of a simple valve equation for flow at the ends of the bed, no axial dispersion and no mass transfer limitations. The equations are discretized using finite difference schemes and then solved using numerical method. For a bed packed with a single adsorbent material and the adsorbent layer say divided into 15 divisions for spatial discretization, Table 2 gives the relation of the number of components with the number of simultaneous, nonlinear algebraic equations to be

Table 2 Number of simultaneous equations to be solved for each time increment as a function of number of components (N)

N	Equations	Comments in respect of PSA process simulation and experiment
2	94	Binary mixtures are widely covered in published work.
3	125 (33% more)	Ternary mixtures are relatively less reported than binary type.
4	156	Present work considers NG treatment with 4 pseudo-components.
5	187	Present work considers NG treatment with 5 pseudo-components.
6	218	The reported system is that for H_2 purification. Present work considers the NG treatment system which may have actually 30 components (Brown et al. 2009).
≥7	≥249	Not found, however patent example gives a process design considering 19 components (Holcombe et al. 1990).

solved in the adsorption step. Computational effort in simulation is thus strongly dependant on the number of components to be handled. Lumping of real components, resembling in some behavior, to form a pseudo-component should therefore help. At the same time, if not done carefully, lumping can alter the phenomenological nature of adsorption/desorption and reflect on simulation quality and its relevance to design/operation decisions. The work done uses minimum amount of input data considering that accounting for non-isothermal behavior and mass transfer limitations will need more input data.

3.1 The model performance

The model performance parameters for a given design and operating conditions used in this work are:

(1) Recovery of undesired components from the feed gas which is defined as the moles of undesired components obtained in the extract per mole of undesired component freshly fed.
(2) Purity is considered to be the mole fraction of desired product in the raffinate over a complete cycle. Propane, Butane and Carbon Dioxide are undesired components on a non-lumped basis. These are calculated as per (1) and (2).

$$\%\ RECOVERY\ of\ Component\ i = \frac{\int_{t=t_1+t_2}^{t=t_{cycle}} (uPy_i)_{z=0}^{t} dt}{\int_{t=0}^{t=t_1+t_2} (uPy_i)_{z=0}^{t} dt} 100 \quad (1)$$

$$\%\ PURITY\ of\ Component\ k = \frac{\int_{t=t_1}^{t=t_1+t_2+t_3} (uPy_k)_{z=L}^{t} dt}{\int_{t=t_1}^{t=t_1+t_2+t_3} (uP)_{z=L}^{t} dt} 100 \quad \text{where } k \neq i \quad (2)$$

4 Heuristics in the assignment of pseudo-components in study of adsorptive separations

The manner of lumping of components in adsorption is not generalized so far (Annesini et al. 1994). Adsorptive separation systems are mainly of three types; (i) TSA, (ii) PSA, VSA, PVSA and (iii) SMB. Typically the first type is operated as 4 step-cycles. The second type cycles have 4–10 steps and the last one consists of 4–6 sections rather than steps. It is to be noted that the simulation model used in the present work is for the second type of adsorptive separation system. The models for the remaining two types could differ from this type. Ideally the approach to lumping should be developed on a case to case basis, depending on the system as well as the objective of separation. A comparative survey of the heuristics in reported cases is given next in Table 3.

Explicit comparisons or analysis of the PSA cycle simulation results obtained by lumping of components with those obtained by non-lumping of components are not found in the literature. A limited number of systems are found where lumping into pseudo components is incorporated and it is observed that these systems had some common criteria for lumping of components. Isotherm models other than Freundlich or Langmuir for pure components and IAST or Extended Langmuir isotherm for multi-component adsorption were not considered with reported component lumping efforts. The reported feed concentrations of the lumped components are also very low. Lumping based on mass transfer rates remains to be studied in terms of differentiating between equilibrium separations and kinetic separations.

In the present work, findings are reported for a complete PSA cycle simulation for a 6-component NG feed based on 6 different strategies of lumping ($N_r = 6$). These are discussed in the next two sections.

5 Data used for simulation

5.1 Pure component adsorption isotherms

Reported pure component isotherms at the operating temperature of 303.15 K for the adsorption of hydrocarbons and CO_2 on Silica Gel were fitted to a pure component Langmuir isotherm model (Olivier and Jadot 1997). The fitted isotherm parameter values are deemed to be valid for the range of the pressure values used in the pure component experiments. The partial pressures encountered in our cycle are within the range of pressures at which the pure component isotherm parameters were measured. However, it is also assumed that the respective isotherm parameters are valid even if the partial pressures encountered in the cycle are outside the range of pressures used for pure component adsorption isotherm generation.

The fitted values of the parameters are given in Table 4. The value of the parameter b is indicative of the equilibrium selectivity of the adsorbent towards these components as well as the non-linearity of the isotherm. A smaller value of b signifies lower adsorption capacity and higher linearity of isotherm. Pure n-Butane has the highest value of the monolayer saturation capacity which is 63% higher than that of pure Methane but its equilibrium constant is the second highest. Methane is the weakest adsorbate. Pure Propane and pure Carbon Dioxide have nearly same adsorption isotherm parameters. Partial pressure of Methane in the feed is around 3200 kPa. Its adsorption capacity in pure form at this pressure is equal to the adsorption capacity of pure n-Butane at 64 kPa or pure i-Butane at 100 kPa.

Table 3 A comparative survey of heuristics in the use of pseudo-components in simulation of adsorptive separations

System	Process stream (*phase*), cycle type, N_{max} and N_s	Lumping done for cycle	N_r	Remarks
1	Separation of Xylene isomers using zeolites (*l*), SMB, 8 and 4	–	–	Only the three Xylene isomers, desorbent and Ethyl Benzene are considered without any lumping (Minceva and Rodrigues 2002, 2007).
2	H_2 purification from various feed gases using layered bed (*g*), PSA, 6 and 10	–	–	At least four components are considered and the components differ from each other in their chemical properties (Yang and Lee 1998; Lee et al. 1999; Park et al. 2000; Jee et al. 2001). This system uses layered bed. The use of pseudo-components may be undesirable considering the tight quality requirements and high sensitivity of the economics to the recovery (Sircar and Golden 2000; Sircar 2006).
3	H_2 purification from various feed gases using zeolite 5A (*g*), PSA, 6 and 6	no	1	N_2 and CO show very similar isotherms on zeolite 5A and have been treated as a single component (Yang and Lee 1998). Comparison with non-lumped case was not done. A complete cycle was run. These two components also have the same molecular weights.
4	Air separation using zeolites (*g*), PSA or VSA, 5 and 4	yes	1	Air was taken as a mixture of N_2 and a pseudo-component formed by lumping Ar and O_2 for adsorption on zeolites in pure O_2 production due to their same value of Langmuir adsorption isotherm equilibrium constants (Cruz et al. 2005). No comparison of cycle performance with non-lumped case is reported. Most authors consider Air as a binary mixture of O_2 and N_2 (Sun et al. 1996; Nilchan and Pantelides 1998).
5	Air drying using Silica Gel (*g*), PSA, 5 and 6	no	–	Moisture was also considered along with O_2 and N_2 (Chihara and Suzuki 1983; Liu et al. 1998).
6	Pretreatment of Air fed to cryogenic unit (*g*), PSA or TSA, 5 and 6	no	–	Ppm levels of CO_2 and Moisture were considered with N_2 (Rege et al. 2001). Solid was zeolite or layers of alumina and zeolite.
7	CO_2 Capture from power plant flue gas emissions (*g*), PSA or VSA or PVSA, 6 and 9	no	–	Most consider a binary mixture of 13% CO_2 and rest N_2 (Chang et al. 2004; Harlick and Tezel 2004; Ko et al. 2005; Li and Tezel 2007; Zhang et al. 2008). Efforts to gather multi-component adsorption data for flue gas considering CO_2, N_2, O_2, SO_x , NO_x and H_2O is reported but no cycle simulation has been carried out (Mello and Eic 2002; Reynolds et al. 2005; Li et al. 2009; Zhang et al. 2009). A guard bed or a pretreatment bed is used for removal of components likes H_2O, H_2S, CO_2, and SO_2 (Yang and Lee 1998).
8	Separation of linear and branched alkanes (*l*, *g*), SMB/PSA, 19 and 6	no	–	Three, four, eight and nineteen components have been considered for this system on zeolite 5A adsorbent (Holcombe et al. 1990; Minkkinen et al. 1993; Mazzotti et al. 1996; Silva and Rodrigues 1998; Silva et al. 2000).
9	Waste water treatment (*l*), TSA, 41 and 4	no	2	The lumping was done based on members of a pseudo-component (i) obeying the same isotherm and having equal or within an order of magnitude close isotherm parameters and (ii) in addition to (i), solid phase mass transfer coefficients are within the same order of magnitude (Calligaris and Tien 1982; Mehrotra and Tien 1984; Ramaswami and Tien 1986). Isotherm parameters and mass transfer coefficients of a pseudo-component were taken as (i) arithmetic average and (ii) concentration weighted average for unequal initial concentrations of those of its member components (TOC in range of 0.1–400 mg /litre). Comparison between lumped and non-lumped cases was restricted to breakthrough curves and adsorption isotherm. Selective lumping and lumping all the organic impurities into a single pseudo component were also studied and compared. Pure components obeyed Freundlich isotherm and IAST was used to predict multi-component adsorption equilibria. The adsorbent was granular Activated Carbon.
10	Terpenes found in Citrus peel oils + CO_2 (*scf*), PSA, 14 and 6	no	2	Thirteen components (Combined mass fraction in the range of 1.5%–9%) were lumped into 4 pseudo-components in accordance with overlap of breakthrough curves and the chemical structure (Reverchon et al. 1998). These were used for the modeling of breakthrough curves only. Pure component isotherm on Silica Gel was Langmuir and multi-component adsorption was represented by Extended Langmuir with two interaction parameters. Isotherm Parameter values for the pseudo-components were taken as mean of pure component values of the member components. Earlier experiments done on adsorption and desorption breakthrough of the same feed revealed that no mass transfer resistances were involved enabling the use of equilibrium controlled process for the modeling. Same values of interaction parameters were used for all the pseudo-components.

Table 4 Fitted values of pure component Langmuir adsorption isotherm parameters on Silica Gel at 303.15 K

i	Component formula	b_i (m^3/mole)	q_{max} (moles adsorbed/m^3 solid)
1	C_3H_8	0.008400	9091
2	n-C_4H_{10}	0.014970	12771
3	i-C_4H_{10}	0.019770	8019
4	CO_2	0.006400	9470
5	C_2H_6	0.002500	9009
6	CH_4	0.000550	7812

5.2 Feed composition and lumping criteria

Two typical industrial feed gas compositions were used in our studies. For each composition, six cases were simulated. As given in Table 5, Case 1 uses the first feed composition and considers no pseudo-components. Similarly, as given in Table 6, Case 7 uses the second feed composition and considers no pseudo-components. The first feed composition has mass fraction of 5% for C_{2+} and CO_2 whereas the second feed composition has mass fraction of 19% for C_{2+} and CO_2. The viscosity for both the feed compositions at the operating temperature was taken to be 0.000012 Pa·s.

The number of pseudo-components can range from minimum of two to a maximum of five by considering various rough criteria like: (i) desired product, (ii) the ratio of mole fraction of the desired product to the mole fraction of undesired/other product in the feed mixture, (iii) equality in molecular weights, (iv) nearness in the values of pure component adsorption isotherm equilibrium constants, (v) equality in number of Carbon atoms and (vi) considering the chemical nature of the components of the feed NG mixture keep a distinct identity for inorganics, organic isomers and organic non-isomers with same number of C atoms. The number of pseudo-components created by applying the above criteria is given in Table 7. The same is provided as a flow-chart in Fig. 11 in Appendix. In this table, Cases 2 to 6 and Cases 8 to 12 consider pseudo-components for first and second feed compositions respectively using various criteria.

Thus for example, in Case 2 and Case 8, by applying criteria (i-a) and (ii) Methane and Ethane are grouped into the first pseudo-component and the remaining four components are grouped into the second pseudo-component. Similarly by applying criteria (i-b) and (ii), Case 3 and Case 9 again use two pseudo-components but lump Ethane, Carbon Dioxide, Propane and Butanes into one pseudo component. All the hydrocarbons may be lumped into a pseudo-component and CO_2 could be the other component if CO_2 is the only desired product which is an unlikely case. If normal alkanes are the desired product then they can be lumped into a pseudo-component, i-Butane and CO_2 will be the remaining two separate components. This is also an unlikely case.

The components to be considered in the calculation of recovery and purity will also change depending upon the lumping criteria. More details of the lumped cases, the member components of a pseudo-component and the pseudo-component properties are summarized in Tables 8, 9.

Additional calculations that arise in the lumping strategy are the estimation of parameters of isotherm and molecular weights for the pseudo-components based on the values for the member components. The philosophy used for these is given below.

The monolayer saturation capacity was taken to be the same for all the components to maintain the thermodynamic consistency of the Extended Langmuir multi-component adsorption isotherm. The value of this capacity for each feed composition was estimated to be the weighted average of the monolayer capacity of pure components as per (3) because the initial concentrations of the feed gas components were unequal. This means that the pseudo-components will be specified by their mass or mole fractions, molecular weights and adsorption equilibrium constants.

$$q_{max} = \sum_{i=1}^{6} (q_{i,max} w_i) \tag{3}$$

where w_i is the mass fraction of ith component.

For the estimation of adsorption equilibrium constant of the pseudo-components, again weighted average of pure component adsorption equilibrium constants was used. Sample calculation as per the two equations below is made for Case 2 or Case 8.

$$b_1 = \frac{b_5 w_5 + b_6 w_6}{w_5 + w_6}, \tag{4}$$

$$b_2 = \frac{\sum_{i=1}^{4} [b_i w_i]}{\sum_{i=1}^{4} w_i} \tag{5}$$

The molecular weight of pseudo-components was determined as per the two equations given below.

$$\mathrm{MW}_1 = \frac{\mathrm{MW}_5 n_5 + \mathrm{MW}_6 n_6}{n_5 + n_6}, \tag{6}$$

$$\mathrm{MW}_2 = \frac{\sum_{i=1}^{4} [\mathrm{MW}_i n_i]}{\sum_{i=1}^{4} n_i} \tag{7}$$

where n_i denotes the number of moles of ith component. Accordingly, the equilibrium constants and molecular weights of pseudo-components used in the remaining cases were found.

From Table 8, it is observed that Case 2 and Case 3 have the same number of pseudo-components but the member components are different. Hence there are differences

Table 5 Case 1: non-lumped 1st feed NG composition ($N_{PC} = 0$)

i	Component formula	Mole fraction	Molecular weight (kg/kmole)	Weight fraction	b_i @ 303.15 K (m^3/mole)	q_{max} @ 303.15 K (moles adsorbed/m^3 solid)
1	C_3H_8	0.0065	44	0.0171	0.008400	7925.4
2	n-C_4H_{10}	0.0011	58	0.0038	0.014970	7925.4
3	i-C_4H_{10}	0.0010	58	0.0035	0.019770	7925.4
4	CO_2	0.0074	44	0.0194	0.006400	7925.4
5	C_2H_6	0.0188	30	0.0337	0.002500	7925.4
6	CH_4	0.9652	16	0.9225	0.000550	7925.4

Table 6 Case 7: non-lumped 2nd feed NG composition ($N_{PC} = 0$)

i	Component formula	Mole fraction	Molecular weight (kg/kmole)	Weight fraction	b_i @ 303.15 K (m^3/mole)	q_{max} @ 303.15 K (moles adsorbed/m^3 solid)
1	C_3H_8	0.0364	44	0.0866	0.008400	8309.6
2	n-C_4H_{10}	0.0223	58	0.0699	0.014970	8309.6
3	i-C_4H_{10}	0.0068	58	0.0213	0.019770	8309.6
4	CO_2	0.0018	44	0.0043	0.006400	8309.6
5	C_2H_6	0.0148	30	0.0240	0.002500	8309.6
6	CH_4	0.9179	16	0.7939	0.000550	8309.6

Table 7 Lumping criteria applied on the two feed compositions and number of pseudo-components (N_{PC}) formed in each case

Case	2 and 8	3 and 9	4 and 10	5 and 11	6 and 12
N_r	2	2	2	2	1
Lumping rule	(i-a) Desired product is $C_1 + C_2$ and (ii) Ratio of sum of mole fractions of $C_1 + C_2$ to the sum of mole fractions of $C_3 + C_4 + CO_2$ in feed is more than 15	(i-b) Desired product is pure C_1 and (ii) Ratio of mole fraction of C_1 to the sum of mole fractions of $C_2 + C_3 + C_4 + CO_2$ in feed is more than 15	(iii) Equality of molecular weights and (iv) Almost equal values of adsorption isotherm parameters	(i-c) $C_1 + CO_2$ is the desired product and (v) Equality of C atoms	(vi) Keep distinct identity for Inorganics, organic non-isomers with same no. of C atoms and isomers
N_{PC}	2	2	4	4	5

in molecular weights and isotherm parameters. From Table 8 and Table 9, it is seen that Case 3 and Case 9 have the same number of pseudo-components and the member components of respective pseudo-component are also same. But the properties of the pseudo-components differ due to difference in the feed compositions.

5.3 Other input data used for the simulation

These are given in Tables 10, 11, 12 respectively. The bed dimensions, operating pressures, temperature and cycle step-times used in this work are typical of industrial scale units. The increments along time and space used for the discretization of the differential equations in the model were successively reduced to ensure the convergence of results. Convergent step sizes were established as given in Table 12 such that any further reduction would not change the concentration profiles along bed at any time and concentration against time profiles at any position in the bed.

All simulations were done on the same computer machine with typical specification speed of 1.6 GHz and 1 GB RAM. The machine and the operating system were both 32 bit. The CPU time is a function of number of equations to be solved over each time increment (thus related to the number of components and divisions used for spatial discretization), number of calls to the solver (related to the number of divisions used for temporal discretization), the required accuracy and the number of iterations required for convergence in each call. For a step of the PSA cycle, temporal step size was kept fixed. The CPU time included typical book-keeping and input/output operations but was dominated by the time required to solve the equations.

The governing model equations are mass conservation equations. However the number crunching is so intensive that truncation and round-off errors could affect the sanctity of the result. Overall mass balances were checked across

Table 8 Member components and their properties for the lumped cases with 1st feed composition at 303.15 K

Case	Pseudo-component	Member components	Mole fraction	Molecular weight kg/kmole	b_i m^3/mole
2	1	C_1 and C_2	0.984	16.27	0.0006
	2	C_3, i-C_4, n-C_4 and CO_2	0.016	45.79	0.0089
3	1	C_1	0.9653	16	0.00055
	2	C_2, C_3, i-C_4, n-C_4 and CO_2	0.0347	37.22	0.006121
4	1	C_1	0.9654	16	0.00055
	2	C_2	0.0188	30	0.0025
	3	C_3 and CO_2	0.0138	44	0.007334
	4	n-C_4 and i-C_4	0.002	58	0.017233
5	1	C_1 and CO_2	0.9727	16.21	0.00067
	2	C_2	0.0188	30	0.0025
	3	C_3	0.0065	44	0.0084
	4	n-C_4 and i-C_4	0.002	58	0.017233
6	1	C_1	0.9653	16	0.00055
	2	C_2	0.0188	30	0.0025
	3	C_3	0.0065	44	0.0084
	4	n-C_4 and i-C_4	0.002	58	0.017233
	5	CO_2	0.0074	44	0.0064

Table 9 Member components and their properties for the lumped cases with 2nd feed composition at 303.15 K

Case	Pseudo-component	Member components	Mole fraction	Molecular weight kg/kmole	b_i m^3/mole
8	1	C_1 and C_2	0.9327	16.22	0.000607
	2	C_3, i-C_4, n-C_4 and CO_2	0.0673	50.05	0.012209
9	1	C_1	0.9178	16	0.00055
	2	C_2, C_3, i-C_4, n-C_4 and CO_2	0.0822	46.42	0.01107
10	1	C_1	0.9178	16	0.00055
	2	C_2	0.0149	30	0.0025
	3	C_3 and CO_2	0.0382	44	0.008306
	4	n-C_4 and i-C_4	0.0291	58	0.016092
11	1	C_1 and CO_2	0.9196	16.05	0.000581
	2	C_2	0.0149	30	0.0025
	3	C_3	0.0364	44	0.0084
	4	n-C_4 and i-C_4	0.0291	58	0.016092
12	1	C_1	0.9178	16	0.00055
	2	C_2	0.0149	30	0.0025
	3	C_3	0.0364	44	0.0084
	4	n-C_4 and i-C_4	0.0291	58	0.016092
	5	CO_2	0.0018	44	0.0064

the bed over each step of any PSA cycle and over the entire cycle. The relative errors were more for strongly adsorbed components as compared to weakly adsorbed components. Suitable choice of time and space discretization and weights assigned for equation residuals could help restrict the mass balance error within tolerance. The residuals of each equation were studied at several stages of solutions for their orders of magnitude and suitable scalar multipliers were incorporated into the corresponding equations to approximately match the orders. This not only speeded up convergence but also reduced mass balance closure errors to a significant extent.

Table 10 Adsorbent, bed and valve properties used in the simulation

Sphericity	1
Particle diameter (mm)	2
Bed voidage	0.35 (Malek and Farooq 1997)
Inner diameter of bed (m)	1.5
Adsorbent height (m)	7
Flow coefficients	
Feed valve	0.01
Raffinate valve	0.00029
Extract valve	0.0038 (0.004 for lumped case)
Purge valve	0.006

Table 11 Operating conditions of the simulated cycle

Adsorption temperature (K)	303.15
Pressures (Pa-absolute $\times 10^{-5}$)	
Feed tank	34
Raffinate tank	21
Extract tank	5.5
Purge tank	7.5
Cycle step duration (s)	
t_1	10
t_2	560
t_3	16
t_4	38
t_5	61
t_{cycle} (s)	685

Table 12 Numerical solver related data

dz (m)	0.47
dt (s)	
Step 1	0.10
Step 2	1.00
Step 3	0.10
Step 4	0.50
Step 5	1.00
Step size for Jacobian	0.001 (El-Hawary and Landrigan 1982)
Estimate of Euclidean distance of the solution from the initial estimate	100 (El-Hawary and Landrigan 1982)
Accuracy requirement	0.01
Max number of iterations	600000

6 Results & discussion

The simulations start with same initial conditions with the bed saturated with one of the pure or pseudo-components as discussed in Sect. 2.1. The cycles are simulated till the bed performance reaches CSS.

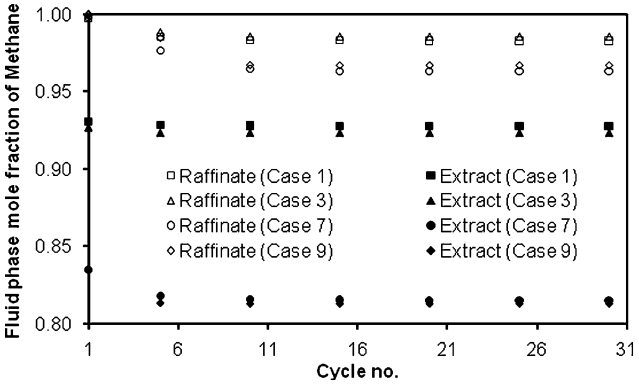

Fig. 2 CSS achievement for Case 1, Case 3, Case 7 and Case 9

6.1 Achievement of CSS

The time averaged mole fraction of components in the extract and the raffinate (purity) after every cycle are calculated for all the cases. When cyclic steady state is attained, the mole fractions in each stream will attain a constant value. The plots from Fig. 2 show that cyclic steady state is achieved within 20 cycles for the four cases as thereafter the curves remain flat. The same observation holds true for the remaining cases. One would have expected CSS achievement in fewer cycles in case of smaller number of true or pseudo-components. This is not supported by the simulation findings, at least in the range of number of such components that we studied. Compared to the feed composition used in Case 1 and Case 3, the feed composition used in Case 7 and Case 9 has 4.2 times higher mole fraction of the stronger adsorbates. But the simulation findings show no effect of the content of the stronger adsorbates on achievement of CSS.

6.2 Concentration profiles of the components in fluid and the solid phases at CSS for feed compositions used in Case 1 and Case 7

The fluid phase mole fractions (see Fig. 3 & Fig. 4) and solid phase concentrations (see Fig. 5 and Fig. 6) at CSS have been plotted for the component that has the highest adsorption equilibrium constant (i-Butane) and for the component that has the lowest adsorption equilibrium constant (Methane) respectively. These are taken at various positions along the adsorbent layer and at a time near the end of each step of the cycle. Thus profiles at 9 s, 569 s, 585 s, 623 s and 684 s represent the profiles near the end of Step 1, Step 2, Step 3, Step 4 and Step 5 respectively. A raffinate stream having lesser content of the strongly adsorbed components than that in the feed gas is produced for both the feed compositions. These four figures also show the effect of changing the feed composition on the separation performance. Compared to the 1st feed composition, the 2nd feed composition has higher content of strongly adsorbed components and so

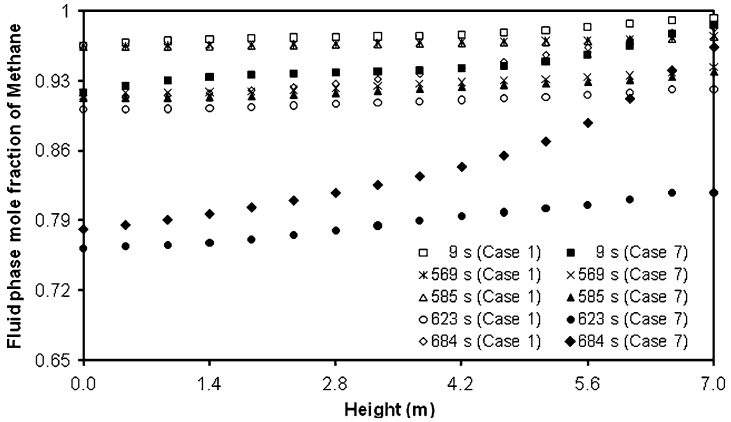

Fig. 3 Fluid phase mole fraction of Methane for Case 1 and Case 7 at different spatial locations along the adsorbent layer near the end of each step of the cycle

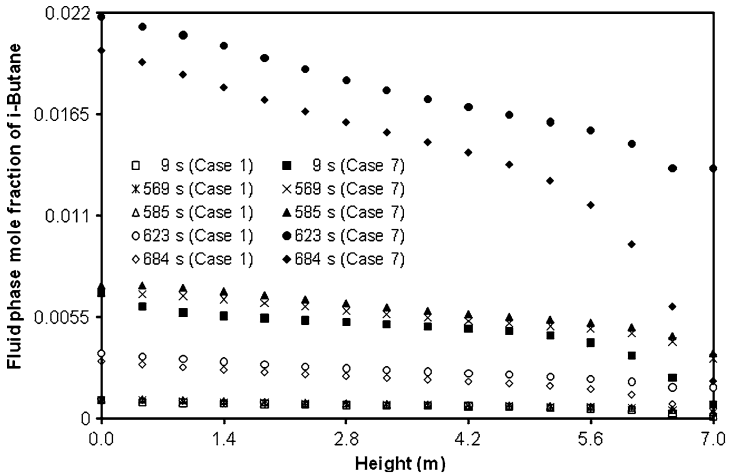

Fig. 4 Fluid phase mole fraction of i-Butane for Case 1 and Case 7 at different spatial locations along the adsorbent layer near the end of each step of the cycle

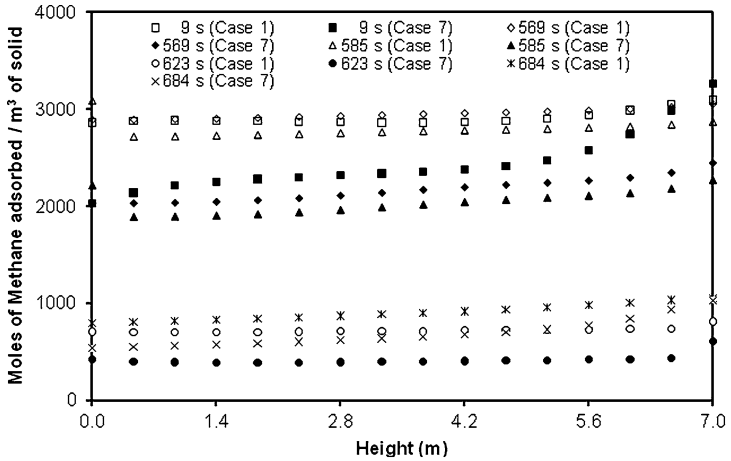

Fig. 5 Solid phase mole concentration of Methane for Case 1 and Case 7 at different spatial locations along the adsorbent layer near the end of each step of the cycle

for the same step times and bed dimensions, gives a 5% to 6% lesser recovery of these components. The recovery can be increased by changing the time of adsorption step and the purge step.

The behavior is same for both the feed compositions and typical of pressure swing based adsorptive separations (Rege et al. 2001; Ribeiro et al. 2008). The profiles indicate that the entire bed length is active during all the steps of the cycle for both the feed compositions.

All the simulations being done for identical sizes, cycle configuration, discretization in space and time, etc, the computation effort is thus solely dependent on the number of simultaneous equations to be solved for marching from one instant of time to the next incremental time. That in turn de-

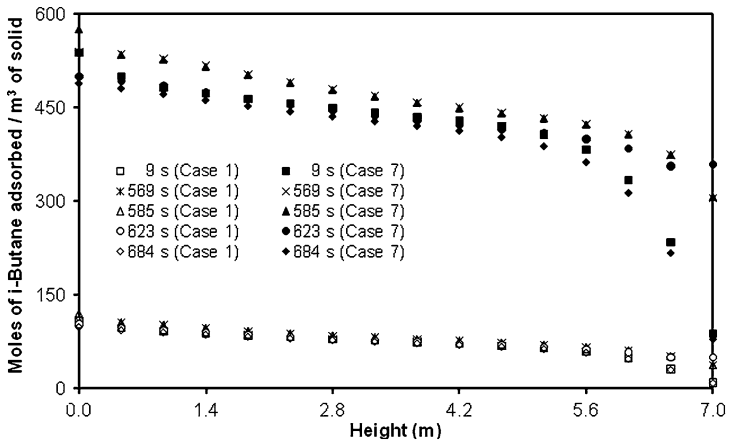

Fig. 6 Solid phase concentration of i-Butane for Case 1 and Case 7 at different spatial locations along the adsorbent layer near the end of each step of the cycle

Table 13 Molecular weights of the streams, number of solved equations, CPU time range and feed rate for each case

Case	MW_{Feed} kg/kmole	$MW_{Raffinate}$ kg/kmole	$MW_{Extract}$ kg/kmole	Equations solved in Step 2 per call to solver	Range of CPU time (s) per cycle	Q_{Feed} (SCMPH)
1	16.74	16.33	17.59	218	313–332	13981
2	16.74	16.44	17.32	94	36–41	14034
3	16.74	16.31	17.62	94	44–79	13993
4	16.74	16.33	17.57	156	88–164	13984
5	16.74	16.47	17.25	156	88–164	14129
6	16.74	16.33	17.58	187	154–220	13983
7	18.50	17.03	21.72	218	325–374	13675
8	18.50	17.11	21.31	94	29–34	13664
9	18.50	17.01	21.68	94	34–60	13674
10	18.50	17.03	21.61	156	111–134	13683
11	18.50	17.08	21.45	156	92–139	13691
12	18.50	17.03	21.61	187	164–237	13674

pends on the number of true or pseudo components as discussed and quantified in Sect. 3.

6.3 Comparison of lumped case with non-lumped case

The pseudo-components of a case differ from the components of a non-lumped case and pseudo-components of other lumped cases in terms of their number, adsorption equilibrium constants and molecular weights. For Case 2, the first pseudo-component has an adsorption equilibrium constant closer to but greater than that of pure Methane and the second pseudo-component has an adsorption equilibrium constant nearly equal to that of pure Propane. Thus, in the lumped cases, a weakly adsorbed component may get grouped into a pseudo-component that has a higher or significantly higher equilibrium constant than the pure component value and a strongly adsorbed component may get grouped into a pseudo-component that has a lower or significantly lower equilibrium constant than the pure component value. The case wise separation performances obtained in the present work show that this discrepancy turns out to be acceptable for the system of NG treatment as the feed gas has trace amounts of strongly adsorbed components and no competitive adsorption behavior among the various adsorbates (Ceresi and Tien 1991).

The molecular weights are used in the calculation of density in the valve equation and the pressure drop equation. Table 13 shows that the variation in the molecular weights of the three streams is very less for this system. The CPU time is estimated for every cycle of a case till CSS was achieved and a range of values for each case is given. As seen in Table 13, for both the feed compositions, CPU time is observed to increase with increase in the number of components. This is as expected. CPU time also depends on the number of iterations required by the solver to return a convergent solution in each call. The more number of iterations means more CPU time and this number may vary from call to call. Hence it is observed that CPU time differs between two lumped cases which have the same number of components and the same feed composition on a non-lumped basis or even dif-

ferent compositions. Table 13 also shows the feed flow rate for all the cases. The difference in the feed flow rates for the lumped case and non-lumped case is within 1%.

For comparing the results of the non-lumped case with that of the lumped case for a particular feed composition, the overall cycle performance in terms of recovery, purity and feed rate values at CSS is taken as the basis for comparison. Additionally the concentration profiles have been made for the purpose of comparison. Now Case 8 and Case 9 have the same number of pseudo-components. However it should be pointed out again that the components considered in the estimation of recovery and purity differ as the member components of the pseudo-component differ from Case 8 to Case 9. For the second feed composition which has a higher content of stronger adsorbates, a comparison of the solid phase concentration profiles for lumped case considering only two pseudo-components (the lowest number) with non-lumped case, is shown in Fig. 7a and Fig. 7b. In Fig. 7a, the sum of the solid phase concentrations of Methane and Ethane obtained from Case 7 is compared with that of the first pseudo-component in Case 8. In Fig. 7b, Methane from Case 7 is compared with Methane from Case 9. The trends are similar and there is a very small difference between Case 7 and Case 8 or between Case 7 and Case 9. Figure 8a and Fig. 8b show the instantaneous mole fraction of a pseudo-component formed by lumping Methane and Ethane in the outgoing fluid from both the ends of the bed over a cycle. These compare Case 7 with Case 8. Tables 14, 15, 16, 17, 18, and Table 19 give the comparison of separation performances of non-lumped case with that of the lumped cases.

Table 14 shows that lumping Methane and Ethane into a pseudo-component and the remaining into a second pseudo-component predicts almost the same separation performance as that of the non-lumped case. This considers the feed

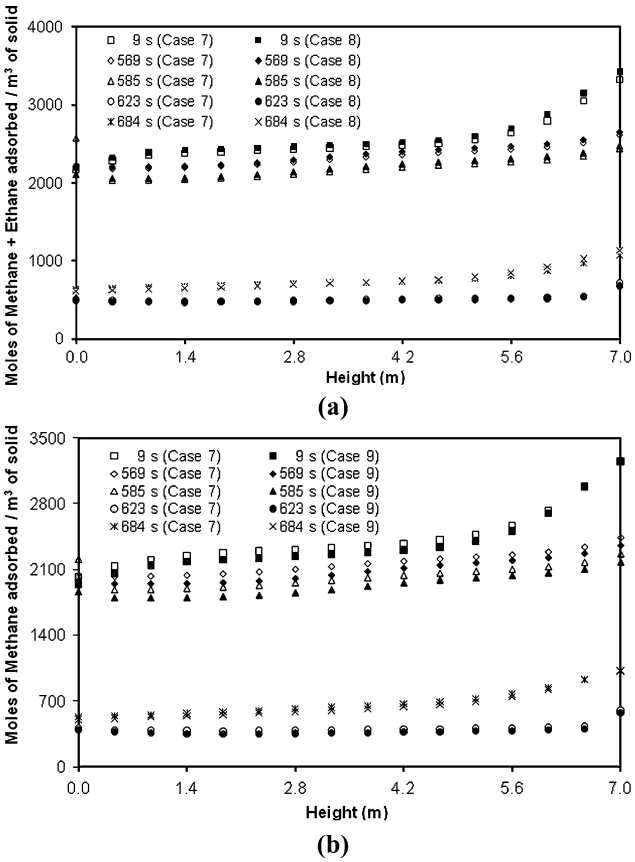

Fig. 7 Comparison based on **(a)** Solid phase concentration of 1st pseudo-component as per Case 8 and with the equivalent sum for non-lumped components as per Case 7 and **(b)** Solid phase concentration of 1st pseudo-component as per Case 9 and with the equivalent non-lumped component as per Case 7 at different spatial locations along the adsorbent layer near the end of each step of the cycle

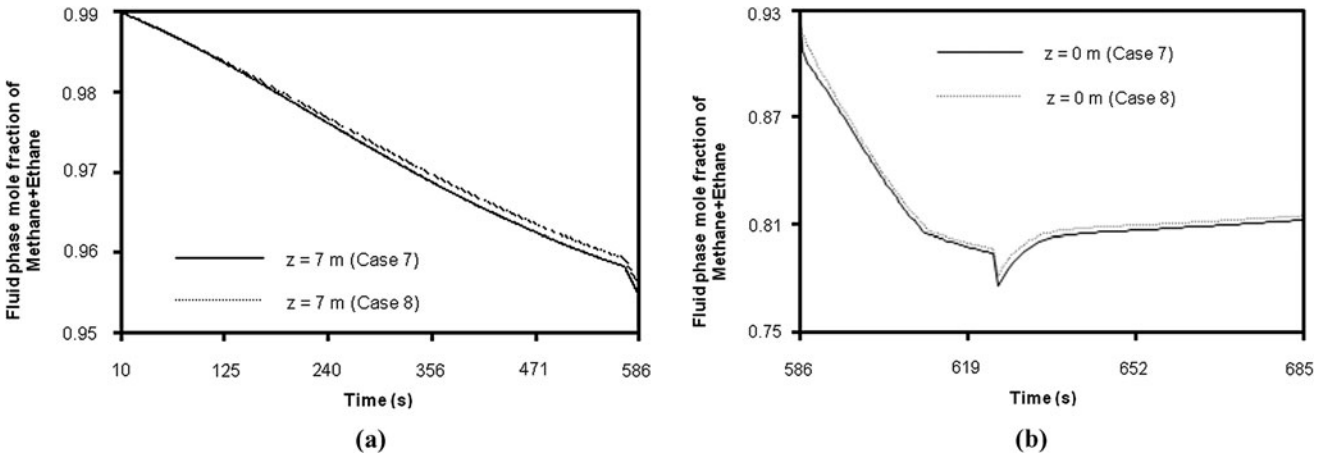

Fig. 8 Instantaneous mole fraction of (**a**) Methane + Ethane in the outgoing fluid stream for Case 7 and Case 8 during adsorption and current depressurization steps and (**b**) Methane + Ethane in the outgoing fluid stream for Case 7 and Case 8 during countercurrent depressurization and purge steps

Table 14 Comparison of Case 2, Case 4 and Case 6 with Case 1

Case	1	2	4	6
% moles of $C_1 + C_2$ in				
Feed	98.42	98.42	98.42	98.42
Raffinate (Purity)	99.40	99.42	99.41	99.40
Extract	96.34	96.45	96.40	96.37
% recovery of $CO_2 + C_{2+}$	69.27	69.79	69.07	69.27

Table 15 Comparison of Case 3, Case 4 and Case 6 with Case 1

Case	1	3	4	6
% moles of C_1 in				
Feed	96.52	96.52	96.52	96.52
Raffinate (Purity)	98.29	98.56	98.30	98.30
Extract	92.80	92.35	92.86	92.82
% recovery of $CO_2 + C_{1+}$	62.71	66.97	62.56	62.71

Table 16 Comparison of Case 5 and Case 6 with Case 1

Case	1	5	6
% moles of $C_1 + C_2 + CO_2$ in			
Feed	99.14	99.14	99.14
Raffinate (Purity)	99.70	99.68	99.71
Extract	97.99	98.13	98.02
% recovery of C_3 + n-C_4 + i-C_4	70.71	69.47	70.72

Table 17 Comparison of Case 8, Case 10 and Case 12 with Case 7

Case	7	8	10	12
% moles of $C_1 + C_2$ in				
Feed	93.27	93.27	93.27	93.27
Raffinate (Purity)	97.37	97.30	97.30	97.30
Extract	84.48	84.94	84.72	84.71
% recovery of $CO_2 + C_{2+}$	64.86	63.93	63.41	63.48

Table 18 Comparison of Case 9, Case 10 and Case 12 with Case 7

Case	7	9	10	12
% moles of C_1 in				
Feed	91.78	91.78	91.78	91.78
Raffinate (Purity)	96.32	96.69	96.31	96.31
Extract	81.54	81.31	82.04	82.04
% recovery of $CO_2 + C_{1+}$	63.16	63.29	60.99	61.06

composition which has lower amounts of Propane, Butanes and CO_2. For the second feed composition, the same lumping strategy predicts almost the same purity but a 2% lower recovery. Table 16 and Table 19 consider only Propane and Butanes in the recovery calculation. The purity values are identical in lumped case and the non-lumped case and the recovery values for the lumped case are up to 2% lower than that in the non-lumped case. The cases with significant deviation are discussed in the next paragraph.

Table 19 Comparison of Case 11 and Case 12 with Case 7

Case	7	11	12
% moles of $C_1 + C_2 + CO_2$ in			
Feed	93.45	93.45	93.45
Raffinate (Purity)	97.39	97.33	97.39
Extract	84.91	85.34	85.10
% recovery of C_3 + n-C_4 + i-C_4	64.79	63.15	63.58

As per Table 15, Case 3 predicts a much higher deviation of 6.3% in recovery value of CO_2 and C_{1+} from that of Case 1. So lumping Ethane with Propane, Butanes and Carbon Dioxide as done in Case 3 turns out to be a bad way of lumping. Moles of this pseudo component collected in the extract are estimated to be 7% more than the corresponding value in Case 1 while those collected in the raffinate are 16% less than the corresponding value in Case 1. The effect of these two differences is an overall difference of 4% more recovery for Case 3. Figure 9a to Fig. 9d show the cause of differences in the performance parameters for these two cases. As seen from these figures, the moles of the pseudo-component collected in the extract for Case 3 are more than those in Case 1 due to higher fluid phase mole fraction of the pseudo-component at the extract end in Case 3. The moles collected in raffinate are lesser due to lesser mole fraction. Again from Table 18, recoveries of CO_2 and C_{1+} in Case 10 and Case 12 are 3% less than that in Case 7 because the instantaneous cumulative mole fraction of CO_2 and C_{1+} coming out during counter-current depressurization step is lower for these cases than that in Case 7. This is seen in Fig. 10a to Fig. 10c.

It can be seen from the comparison tables that the lumping criteria applied here do not seem to have drastic effect on the performance parameters because for a given feed composition, majority of the lumped cases predict nearly the same values of cycle performance parameters as are for the non-lumped case. The recovery calculation that considers CO_2 and C_{1+} showed 3–6% deviations for some lumped cases. Recovery calculations that consider only CO_2 and C_{2+} or only C_{2+} turn out to be better ways than recovery calculations that consider only C_{1+} and CO_2. But this system has no strict target on recovery unlike H_2 purification (Sircar 2006). Finally the case that uses the least number of pseudo-components with less significant adverse effect on prediction of process performance will obviously be preferred. Thus the PSA based separation of six-component

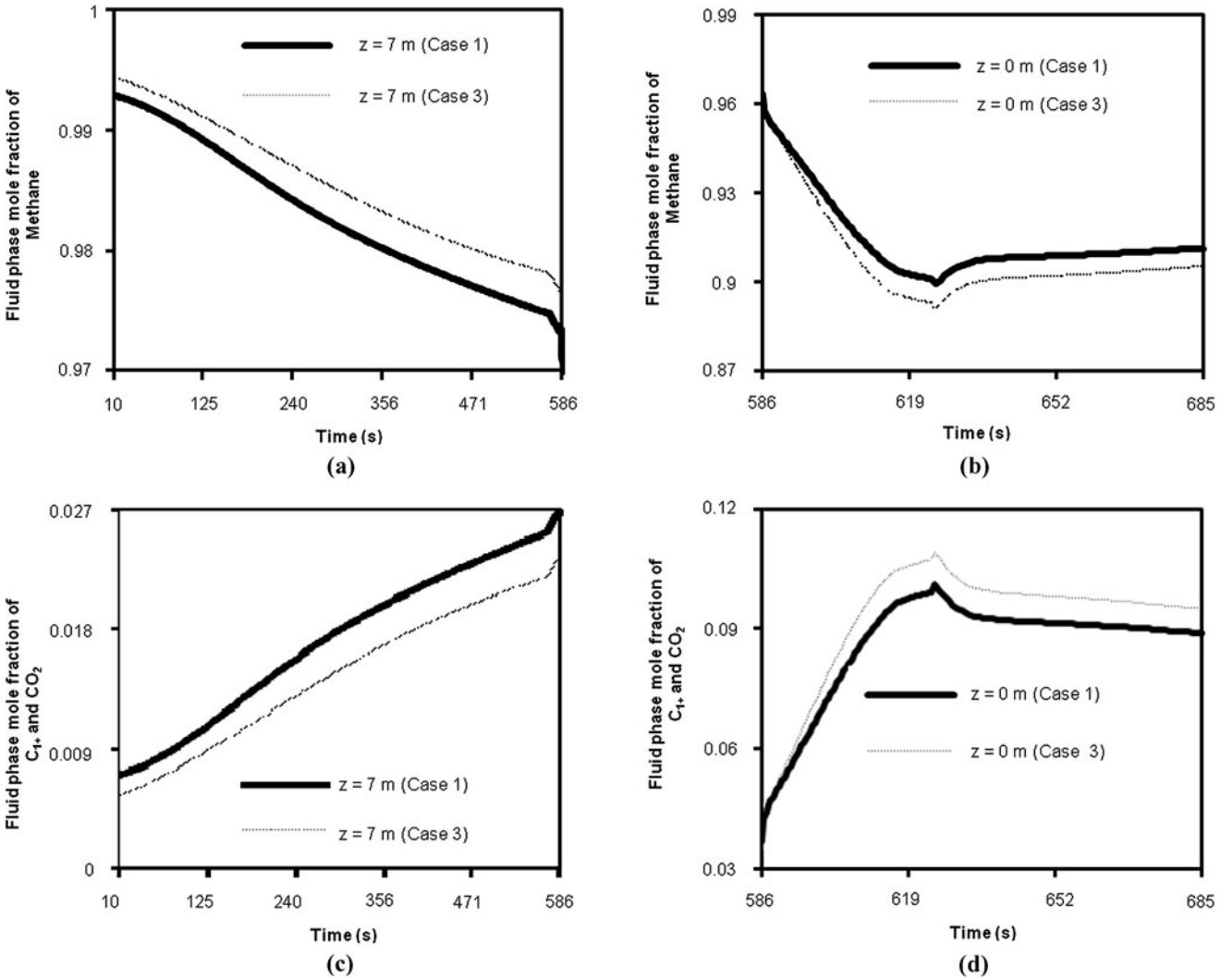

Fig. 9 Instantaneous fluid phase mole fraction in Case 1 and Case 3 of **(a)** Methane at the raffinate end of the bed in adsorption and co-current depressurization steps, **(b)** Methane at the extract end of the bed in counter-current depressurization and purge steps, **(c)** Ethane + Propane + n-Butane + i-Butane + Carbon Dioxide at the raffinate end of the bed in adsorption and co-current depressurization steps and **(d)** Ethane + Propane + n-Butane + i-Butane + Carbon Dioxide at the extract end of the bed in counter-current depressurization and purge steps

mixtures specified by Case 1 or Case 7 can be represented by a mixture of two pseudo-components as specified by Case 2 or Case 8 respectively with sufficient accuracy. This work also serves as a stepwise procedure for arriving at a minimum number of components that will describe with fair accuracy and computational saving, the separation performance of an adsorptive separation cycle involving large number of components.

The stress in the present work was on verifying the validity of lumping true species in fewer pseudo-species so as to significantly reduce the computational effort, but with minimal impact on the phenomenological processes and on performance aspects important from design and operational viewpoints. This demanded proper care in choice of the system details in terms of bed dimensions, number of true species, cycle configuration, pressure levels, flow rates, etc. It was realized that any conclusions drawn based on simulation would lose much of their significance in case of an over designed system. For example, if the adsorber bed is over-designed in the sense that it has a large amount of adsorbent as compared to amount of adsorbing species entering over a cycle step and vying for sorption, the action would be confined to a small part of the bed, with most of the bed not participating to any significant level. The raffinate or extract may thus be not seen significantly different in the case of simulation with lumping versus that with non-lumping. Similar will be the case if the bed is grossly undersized and gets saturated with feed over a smaller part of the step time. The observation can similarly be extended to the duration of each step in a cycle. It is important to select a system in

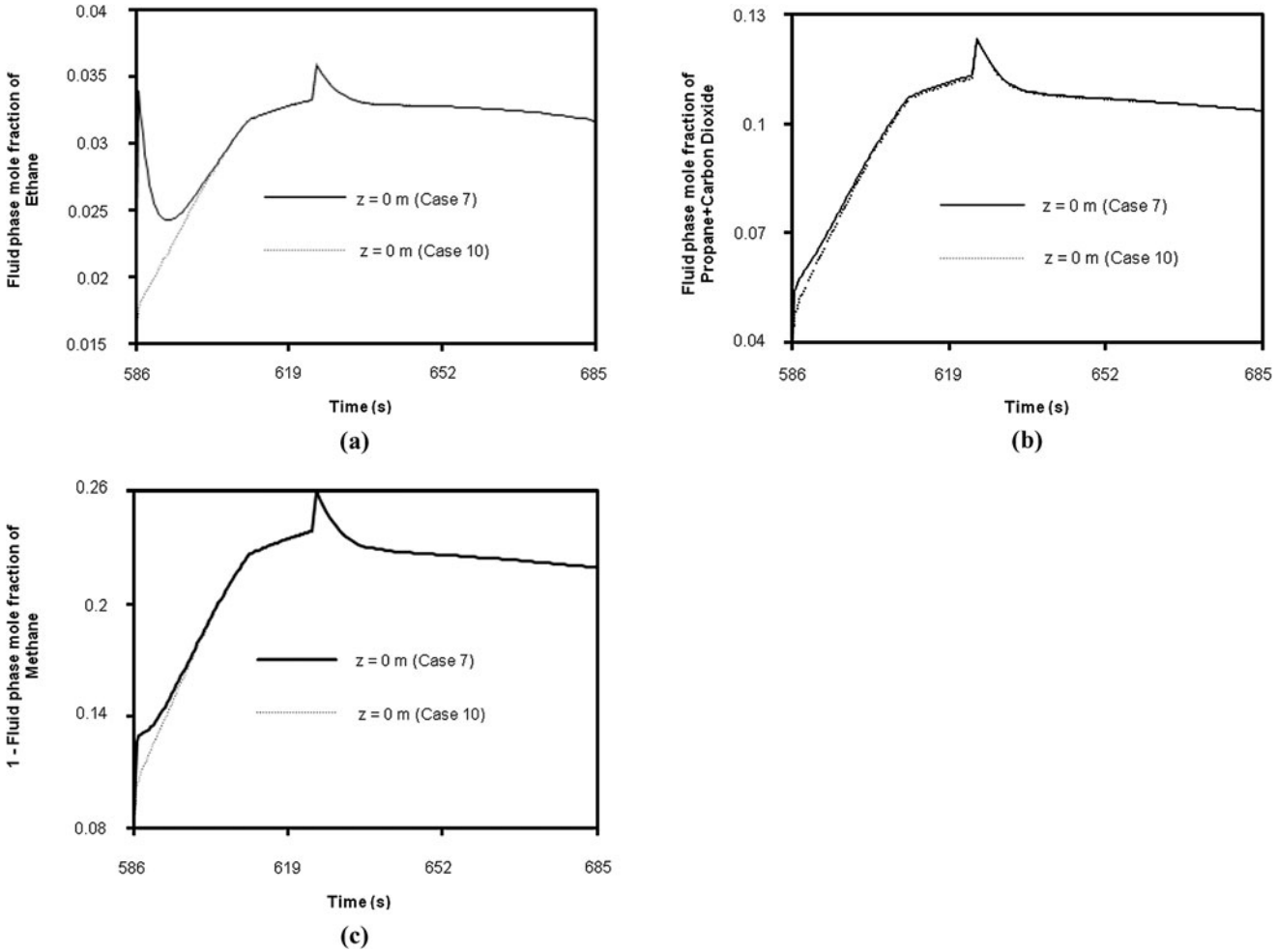

Fig. 10 Instantaneous fluid phase mole fraction in Case 7 and Case 10 for **(a)** Ethane at the extract end of the bed in the counter-current depressurization and purge steps **(b)** Propane + Carbon Dioxide at the extract end of the bed in the counter-current depressurization and purge steps and **(c)** Fluid phase mole fractions of Ethane + Propane + Butanes + Carbon Dioxide at the extract end of the bed in the counter-current depressurization and purge steps

such a way that the entire bed is 'active' during entire duration of each constituent step of a PSA cycle. As discussed earlier, this was checked by observing the component mole fractions along the bed at the end of each step of the cycle. This was done for all cases using different feed composition and different lumping strategies. It was also done for adsorbed phase and bulk phase. Figure 3 to Fig. 10 show profiles of true as well as pseudo-components, dominant as well as least dominant components for different cases. All the plots indicate that the beds are busy in adsorption/desorption in all steps of the PSA cycle and inadequacy of lumping in representing phenomenological aspects will thus be reflected in overall process performance such as purity and recovery.

Optimal industrial system designs will also strive to achieve such designs extracting the maximum out of adsorbent inventory in beds. In fact the results here are from an industrial design carried out using the lumping concept. The design has been implemented in one of the biggest NG treatment plant (8 beds each processing about 10000 m^3/hour of feed gas at STP conditions).

6.4 Effect of variations in operating temperature and cycle step times

Additionally, for the second feed composition, two more variations were studied. Keeping all the other things same, the cycle in Table 11 was first simulated at an operating temperature of 278.15 K. The second variation was carrying out a different cycle at the operating temperature of 303.15 K and keeping the other things same. The isotherm parameters at 278.15 K are given in Table 20 (Olivier and Jadot 1997). The configuration of new cycle is given in Table 21. The adsorption equilibrium constant will increase when the temperature decreases to 278.15 K. This means that the isotherm at 278.15 K becomes more non-linear or more unfavorable

for desorption but more favorable for adsorption and sorption capacity rises compared to that at 303.15 K. To achieve the same separation performance as that at 303.15 K, the adsorption and desorption step times may need to be changed but our emphasis was mainly to study the effect of lumping on separation performance. In non-isothermal operation, the isotherm parameters, transfer coefficients and densities also depend on temperature. Hence to understand the effects of component lumping, isothermal model serves as a better case.

Similarly we have simulated a cycle having different step times for the third and the final steps. This cycle has a lower time and will give a different separation performance than that at 685 s. Naturally the feed rate will increase at the new cycle time. A new step of any cycle is distinguished by its boundary condition and changing the step time or step sequence merely changes the initial condition. Thus decreasing the co-current depressurization step time from 14 s to 2 s will change the bed conditions at the start of countercurrent depressurization step. If the co-current depressurization step time is further reduced to 0 s then also it will mean a different initial condition for countercurrent depressurization. The properties that are affected by component lumping do not change by trying a different cycle which can mean any of i) different steps or ii) different step sequence but same steps or iii) different time of steps but same steps. The required data on the pseudocomponents for these cases is given in Tables 22, 23, 24, 25.

As seen from Table 26 and Table 27, use of two pseudocomponents as per Case 14 and Case 20 is still sufficient to give a fairly accurate separation performance compared to the non-lumped case of six components. The separation performances have changed due to differences in any one of temperature or cycle step times or feed com-

Table 20 Fitted values of pure component Langmuir adsorption isotherm parameters on Silica Gel at 278.15 K

i	Component formula	b_i (m^3/mole)	q_{max} (moles adsorbed/m^3 solid)
1	C_3H_8	0.018196	8696
2	n-C_4H_{10}	0.072667	9174
3	i-C_4H_{10}	0.054032	7463
4	CO_2	0.007286	13072
5	C_2H_6	0.005146	9434
6	CH_4	0.000951	7407

Table 21 New cycle step duration used in Cases 19 to 24

t_1 (s)	10
t_2 (s)	560
t_3 (s)	2
t_4 (s)	38
t_5 (s)	30
t_{cycle} (s)	640

Table 22 Case 13 and Case 19: non-lumped 2nd Feed NG composition ($N_{PC} = 0$)

i	Component formula	Mole fraction	Molecular weight (kg/kmole)	Weight fraction	b_i @ 278.15 K (m^3/mole)	q_{max} @ 278.15 K (moles adsorbed/m^3 solid)
1	C_3H_8	0.0364	44	0.0866	0.018196	7716.4
2	n-C_4H_{10}	0.0223	58	0.0699	0.072667	7716.4
3	i-C_4H_{10}	0.0068	58	0.0213	0.054032	7716.4
4	CO_2	0.0018	44	0.0043	0.007286	7716.4
5	C_2H_6	0.0148	30	0.0240	0.005146	7716.4
6	CH_4	0.9179	16	0.7939	0.000951	7716.4

Table 23 Lumping criteria applied on the second feed compositions and number of pseudo-components (N_{PC}) formed in each case for 1) 278.15 K operating temperature and 685 s cycle time or 2) 640 s cycle time and 303.15 K operating temperature

Case	14 and 20	15 and 21	16 and 22	17 and 23	18 and 24
N_r	2	2	2	2	1
Lumping rule	(i-a) Desired product is $C_1 + C_2$ and (ii) Ratio of sum of mole fractions of $C_1 + C_2$ to the sum of mole fractions of $C_3 + C_4 + CO_2$ in feed is more than 15	(i-b) Desired product is pure C1 and (ii) Ratio of mole fraction of C1 to the sum of mole fractions of $C_2 + C_3 + C_4 + CO_2$ in feed is more than 15	(iii) Equality of molecular weights and (iv) Almost equal values of adsorption isotherm parameters	(i-c) $C_1 + CO_2$ is the desired product and (v) Equality of C atoms	(vi) Keep distinct identity for Inorganics, organic non-isomers with same no. of C atoms and isomers.
N_{PC}	2	2	4	4	5

Table 24 Member components and their properties for the lumped cases with 2nd feed composition at 278.15 K

Case	Pseudo-component	Member components	Mole fraction	Molecular weight kg/kmole	b_i m^3/mole
14	1	C_1 and C_2	0.9327	16.22	0.001074
	2	C_3, i-C_4, n-C_4 and CO_2	0.0673	50.05	0.043053
15	1	C_1	0.9178	16	0.000951
	2	C_2, C_3, i-C_4, n-C_4 and CO_2	0.0822	46.42	0.038625
16	1	C_1	0.9178	16	0.000951
	2	C_2	0.0149	30	0.005146
	3	C_3 and CO_2	0.0382	44	0.017688
	4	n-C_4 and i-C_4	0.0291	58	0.068304
17	1	C_1 and CO_2	0.9196	16.05	0.000984
	2	C_2	0.0149	30	0.005146
	3	C_3	0.0364	44	0.018196
	4	n-C_4 and i-C_4	0.0291	58	0.068304
18	1	C_1	0.9178	16	0.000951
	2	C_2	0.0149	30	0.005146
	3	C_3	0.0364	44	0.018196
	4	n-C_4 and i-C_4	0.0291	58	0.068304
	5	CO_2	0.0018	44	0.007286

Table 25 Member components and their properties for the lumped cases with 2nd feed composition at 303.15 K and cycle time of 640 s (value of q_{max} is given in Table 6)

Case	Pseudo-component	Member components	Mole fraction	Molecular weight kg/kmole	b_i m^3/mole
20	1	C_1 and C_2	0.9327	16.22	0.000607
	2	C_3, i-C_4, n-C_4 and CO_2	0.0673	50.05	0.012209
21	1	C_1	0.9178	16	0.00055
	2	C_2, C_3, i-C_4, n-C_4 and CO_2	0.0822	46.42	0.01107
22	1	C_1	0.9178	16	0.00055
	2	C_2	0.0149	30	0.0025
	3	C_3 and CO_2	0.0382	44	0.008306
	4	n-C_4 and i-C_4	0.0291	58	0.016092
23	1	C_1 and CO_2	0.9196	16.05	0.000581
	2	C_2	0.0149	30	0.0025
	3	C_3	0.0364	44	0.0084
	4	n-C_4 and i-C_4	0.0291	58	0.016092
24	1	C_1	0.9178	16	0.00055
	2	C_2	0.0149	30	0.0025
	3	C_3	0.0364	44	0.0084
	4	n-C_4 and i-C_4	0.0291	58	0.016092
	5	CO_2	0.0018	44	0.0064

position. However changing the operating temperature or changing the cycle step times has not made any drastic effect on finding the minimum required no. of pseudo-components to describe accurately the separation performance for this six component NG feed mixture on Silica gel adsorbent.

7 Conclusions

(1) A mathematical model, assuming isothermal operation and no mass transfer limitations, simulated the treatment of dry NG using Silica Gel as the adsorbent and a 5-step pressure swing adsorption cycle. Extended Langmuir isotherm was used to describe the multi-

Table 26 Results for cycle time of 685 s, 2nd feed composition and operating temperature of 278.15 K

Case	13	14	15	16	17	18
% Moles in raffinate of						
C_1	95.75		96.07	95.74		95.73
$C_1 + C_2$	96.86	96.92		96.86		96.85
$C_1 + C_2 + CO_2$	96.98				96.94	96.97
Range of CPU time (s)/cycle	164–674	16–60	16–42	60–132	60–134	102–202
% Recovery						
$C_{2+} + CO_2$	52.03	51.14		53.37		53.30
$C_{1+} + CO_2$	50.33		50.67	51.45		51.40
C_3 + n-C_4 + i-C_4	52.21				53.40	53.60
Feed rate (SCMPH)	14800	14767	14701	14789	14789	14787

Table 27 Results of cycle time of 640 s, 2nd feed composition and operating temperature of 303.15 K

Case	19	20	21	22	23	24
% Moles in raffinate of						
C_1	95.23		95.5	95.22		95.23
$C_1 + C_2$	96.38	96.42		96.37		96.38
$C_1 + C_2 + CO_2$	96.49				96.44	96.49
Range of CPU time (s)/cycle	229–285	21–33	26–38	70–118	72–124	120–346
% Recovery						
$C_{2+} + CO_2$	49.34	50.24		49.39		49.38
$C_{1+} + CO_2$	47.66		49.54	47.71		47.7
C_3 + n-C_4 + i-C_4	49.4				49.25	49.44
Feed rate (SCMPH)	15751	15767	15721	15755	15796	15754

component adsorption. Dry NG was considered as a mixture of mainly six components. Two feed compositions of NG were used. The first feed composition was an industrial feed and the second feed was a hypothetical feed having more content of Propane and Butanes. Each composition was studied using simulation with and without lumping. The predicted performance of a complete cycle has been used for the comparison between the lumped and non-lumped cases. For the lumped and non-lumped cases, the cycle of time 685 s was run using the second feed composition at operating temperatures of 278.15 K and 303.15 K respectively. A cycle of time 640 s at temperature of 303.15 K and second feed composition was also run using lumped and non-lumped cases. We also made a survey on the earlier use of component lumping in adsorption as given in Table 3.

(2) For both the NG feed compositions, the values of recovery and purity for the lumped case are almost the same as that for the non-lumped case irrespective of the lumping criteria and hence the case which uses the least number of lumps will be preferred as time of computation is the least. The least number of pseudo-components for this system is two. We also confirmed this result by trying out a cycle with different step times and a cycle with different operating temperature.

(3) Lumping of components can be used for simulating an entire PSA cycle for gaseous mixtures which are 'continuous'. The problem finally becomes as one of finding the minimum number of pseudo-components that will describe sufficiently accurately the separation performance for the non-lumped large size system in less computation time. For some lumped cases, the definition of performance parameters needs to be modified accordingly.

(4) The present work has illustrated the use of the lumping strategy in terms of reduction in computational time and pointed out the extent of differences in the outcome of the lumped against non lumped models for the complete five-step PSA cycle for a separation process for NG treatment. Sensitivity of the results with respect to feed composition and pressures has also been studied in this work. This has been done using the minimum available amount of input data and has served in designing an actual plant. We have defined six criteria for lumping the components of NG mixture and then calculated the model required properties of the pseudo-components and finally compared the separation performance results with that of a non-lumped case.

Appendix

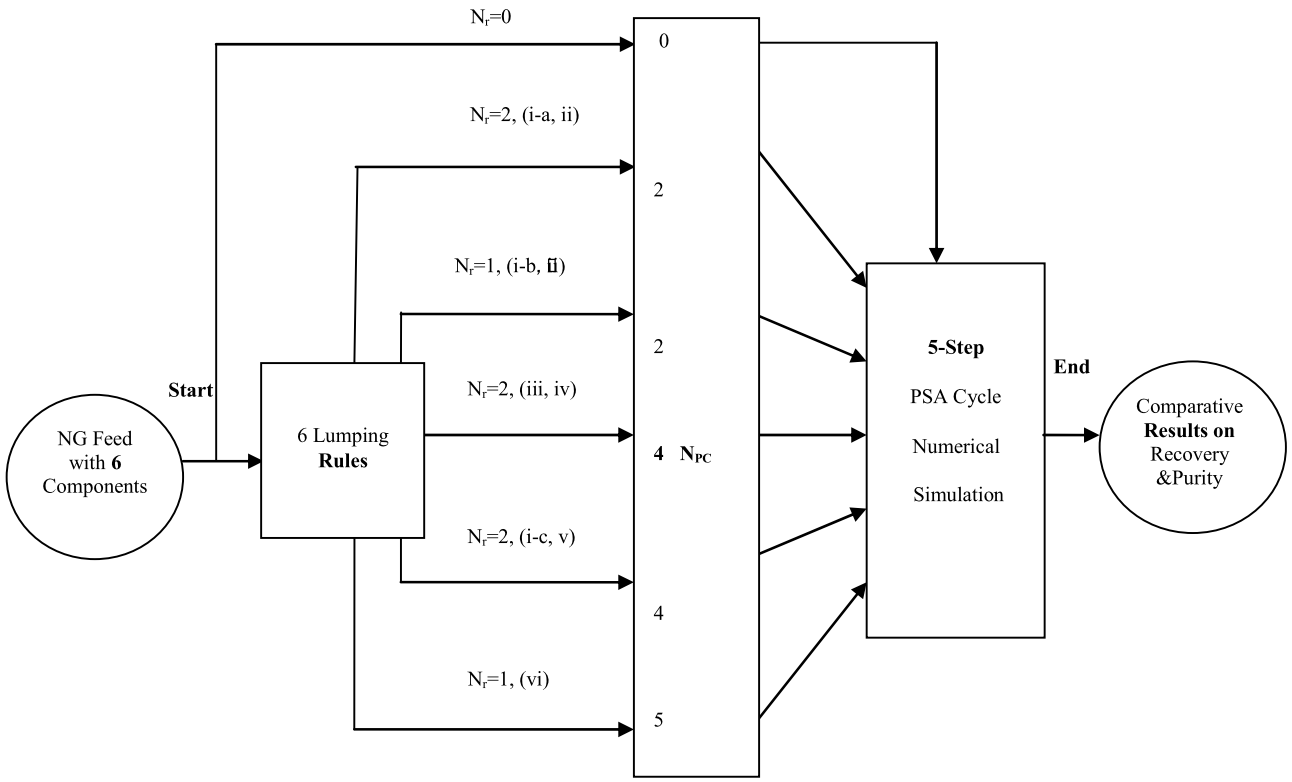

Roman letters in brackets after the N_r value show the rule nos. from the list below:

(i)	Desired product is (i-a) C_1+C_2 or (i-b) C_1 or (i-c) C_1+CO_2	(iv)	Components have almost equal values of adsorption isotherm equilibrium constants
(ii)	Ratio of mole fraction of the desired product to the mole fraction of undesired or other components in the feed is greater than 15	(v)	Components have equal number of C atoms
(iii)	Components have equal values of molecular weights	(vi)	Keep distinct identity for inorganics, organic non-isomers having equal no. of C atoms and isomers

Fig. 11 Flow chart showing the heuristics used in lumping of components in the PSA process for NG separation

References

Annesini, M.A., Giona, M., Gironi, F.: Continuous model for complex mixture adsorption. Ind. Eng. Chem. Res. **33**, 2764–2770 (1994)

Aris, A.: Reactions in continuous mixtures. AIChE J. **35**, 539–548 (1989)

Aris, R., Gavalas, G.R.: On the theory of reactions in continuous mixtures. Philos. Trans. R. Soc. Lond. Ser. A, Math. Phys. Sci. **260**, 351–393 (1966)

Brown, A.S., Milton, M.J.T., Vargha, G.M., Mounce, R., Cowper, C.J., Stokes, A.M.V., Benton, A.J., Lander, D.F., Ridge, A., Laughton, A.P.: Measurement of the hydrocarbon dew point of real and synthetic natural gas mixtures by direct and indirect methods. Energy Fuels **23**, 1640–1650 (2009)

Calligaris, M.B., Tien, C.: Species grouping in multicomponent adsorption calculations. Can. J. Chem. Eng. **60**, 772–780 (1982)

Ceresi, J.E., Tien, C.: Carbon adsorption of phenol from aqueous solutions in the presence of other adsorbates. Sep. Technol. **1**, 273–281 (1991)

Chang, D., Min, J., Moon, K., Park, Y.K., Jeon, J.K., Ihm, S.K.: Robust numerical simulation of pressure swing adsorption process with strong adsorbate CO_2. Chem. Eng. Sci. **59**, 2715–2725 (2004)

Chihara, K., Suzuki, M.: Air drying by pressure swing adsorption. J. Chem. Eng. Jpn. **16**, 293–299 (1983)

Chou, G.F., Prausnitz, J.M.: Adiabatic flash calculations for continuous or semicontinuous mixtures using an equation of state. Fluid Phase Equilib. **30**, 75–82 (1986)

Cruz, P., Magalhães, F.D., Mendes, A.: On the optimization of cyclic adsorption separation processes. AIChE J. **51**, 1377–1395 (2005)

Daiminger, U., Lind, W., Mitariten, M.J.: Adsorption added value. Hydrocarb. Eng. **2**, 83–86 (2006)

El-Hawary, M.S., Landrigan, J.K.: Optimum operation of fixed-head hydro-thermal electric power systems: Powell's hybrid method versus Newton-Raphson method. IEEE Trans. Power Appar. Syst. **101**, 547–554 (1982)

Glinos, K., Malone, M.F.: Minimum reflux, product distribution, and lumping rules for multicomponent distillation. Ind. Eng. Chem. Process Des. Dev. **23**, 764–768 (1984)

Harlick, P.J.E., Tezel, H.F.: An experimental adsorbent screening study for CO_2 removal from N_2. Microporous Mesoporous Mater. **76**, 71–79 (2004)

Holcombe, T.C., Sager, T.C., Volles, W.K., Zarchy, A.S.: Isomerization process. US Patent 4,929,799 (1990)

Jacome, P.A.D., Peixoto, F.C., Platt, G.M., Ahon, V.R.R.: A new approach to distillation of continuous mixtures: modelling and simulation. Lat. Am. Appl. Res. **35**, 233–239 (2005)

Jee, J.G., Kim, M.B., Lee, C.H.: Adsorption characteristics of hydrogen mixtures in a layered bed: binary, ternary, and five-component mixtures. Ind. Eng. Chem. Res. **40**, 868–878 (2001)

Ko, D., Siriwardane, R., Biegler, L.T.: Optimization of pressure swing adsorption and fractionated vacuum pressure swing adsorption processes for CO_2 capture. Ind. Eng. Chem. Res. **44**, 8084–8094 (2005)

Lee, C.H., Yang, J., Ahn, H.: Effects of carbon-to-zeolite ratio on layered bed H_2 PSA for coke oven gas. AIChE J. **45**, 535–545 (1999)

Li, G., Xiao, P., Webley, P.A., Zhang, J., Singh, R.: Competition of CO_2/H_2O in adsorption based CO_2 capture. Energy Procedia **1**, 1123–1130 (2009)

Li, P., Tezel, H.F.: Equilibrium and kinetic analysis of CO_2–N_2 adsorption separation by concentration pulse chromatography. J. Colloid Interface Sci. **313**, 12–17 (2007)

Liu, Y., Delgado, J., Ritter, J.A.: Comparison of finite difference techniques for simulating pressure swing adsorption. Adsorption **4**, 337–344 (1998)

Malek, A., Farooq, S.: Kinetics of hydrocarbon adsorption on activated carbon and silica gel. AIChE J. **43**, 761–776 (1997)

Maurer, R.T.: Methane purification by pressure swing adsorption. US Patent 5,171,333 (1992)

Mazzotti, M., Baciocchi, R., Storti, G., Morbidelli, M.: Vapor-phase SMB adsorptive separation of linear/nonlinear paraffins. Ind. Eng. Chem. Res. **35**, 2313–2321 (1996)

Mehrotra, A.K., Tien, C.: Further work in species grouping in multicomponent adsorption calculation. Can. J. Chem. Eng. **62**, 632–643 (1984)

Mello, M., Eic, M.: Adsorption of sulfur dioxide from pseudo binary mixtures on hydrophobic zeolites: modelling of the breakthrough curves. Adsorption **8**, 279–289 (2002)

Minceva, M., Rodrigues, A.E.: Modeling and simulation of a simulated moving bed for the separation of p-xylene. Ind. Eng. Chem. Res. **41**, 3454–3461 (2002)

Minceva, M., Rodrigues, A.E.: Understanding and revamping of industrial scale SMB units for p-xylene separation. AIChE J. **53**, 138–149 (2007)

Minkkinen, A., Mank, L., Jullian, S.: Process for the isomerization of C_5/C_6 normal paraffins with recycling of normal paraffins. US Patent 5,233,120 (1993)

Nilchan, S., Pantelides, C.C.: On the optimization of periodic adsorption processes. Adsorption **4**, 113–147 (1998)

Olivier, M.G., Jadot, R.: Adsorption of light hydrocarbons and carbon dioxide on silica gel. J. Chem. Eng. Data **42**, 230–233 (1997)

Park, J.H., Kim, J.N., Cho, S.H.: Performance analysis of four-bed H_2 PSA process using layered beds. AIChE J. **46**, 790–802 (2000)

Ramaswami, S., Tien, C.: Simplification of multicomponent fixed-bed adsorption calculations by species grouping. Ind. Eng. Chem. Process Des. Dev. **25**, 133–139 (1986)

Rege, S.U., Yang, R.T.: A novel FTIR method for studying mixed gas adsorption at low concentrations: H_2O and CO_2 on NaX zeolite and γ-alumina. Chem. Eng. Sci. **56**, 3781–3796 (2001)

Rege, S.U., Yang, R.T., Qian, K., Buzanowski, M.A.: Air-prepurification by pressure swing adsorption using single/layered beds. Chem. Eng. Sci. **56**, 2745–2759 (2001)

Reverchon, E., Lamberti, G., Subra, P.: Modelling and simulation of the supercritical adsorption of complex terpene mixtures. Chem. Eng. Sci. **53**, 3537–3544 (1998)

Reynolds, S.P., Ebner, A.D., Ritter, J.A.: New pressure swing adsorption cycles for carbon dioxide sequestration. Adsorption **11**, 531–536 (2005)

Ribeiro, A.M., Grande, C.A., Lopes, F.V.S., Loureiro, J.M., Rodrigues, A.E.: A parametric study of layered bed PSA for hydrogen purification. Chem. Eng. Sci. **63**, 5258–5873 (2008)

Robben, M.A., O'Brien, D.: The case for silica. Hydrocarb. Eng. **8**, 23–28 (2005)

Silva, J.A.C., Rodrigues, A.E.: Separation of n/iso-paraffins mixtures by pressure swing adsorption. Sep. Purif. Technol. **13**, 195–208 (1998)

Silva, J.A.C., Da Silva, F.A., Rodrigues, A.E.: Separation of n/iso paraffins by PSA. Sep. Purif. Technol. **20**, 97–110 (2000)

Sircar, S.: Basic research needs for design of adsorptive gas separation processes. Ind. Eng. Chem. Res. **45**, 5435–5448 (2006)

Sircar, S., Golden, T.C.: Purification of hydrogen by pressure swing adsorption. Sep. Sci. Technol. **35**, 667–687 (2000)

Sircar, S., Hufton, J.R.: Why does the linear driving force model for adsorption kinetics work? Adsorption **6**, 137–147 (2002)

Sun, L.M., Quere, P.L., Levan, M.D.: Numerical simulation of diffusion-limited PSA process models by finite difference methods. Chem. Eng. Sci. **51**, 5341–5352 (1996)

Yang, J., Lee, C.H.: Adsorption dynamics of a layered bed PSA for H_2 recovery from coke oven gas. AIChE J. **5**, 1325–1334 (1998)

Zhang, J., Webley, P.A., Xiao, P.: Effect of process parameters on power requirements of vacuum swing adsorption technology for CO_2 capture from flue gas. Energy Convers. Manag. **49**, 346–356 (2008)

Zhang, J., Xiao, P., Li, G., Webley, P.A.: Effect of flue gas impurities on CO_2 capture performance from flue gas at coal-fired power stations by vacuum swing adsorption. Energy Procedia **1**, 1115–1122 (2009)